

# Isospin-symmetry breaking in superallowed Fermi $\beta$ -decay due to isospin-nonconserving forces

K. Kaneko

*Department of Physics, Kyushu Sangyo University, Fukuoka 813-8503, Japan*

Y. Sun

*School of Physics and Astronomy, Shanghai Jiao Tong University, Shanghai 200240, China*

*Collaborative Innovation Center of IFSA, Shanghai Jiao Tong University, Shanghai 200240, China*

*Institute of Modern Physics, Chinese Academy of Sciences, Lanzhou 730000, China*

T. Mizusaki

*Institute of Natural Sciences, Senshu University, Tokyo 101-8425, Japan*

S. Tazaki

*Department of Applied Physics, Fukuoka University, Fukuoka 814-0180, Japan*

S. K. Ghorui

*School of Physics and Astronomy, Shanghai Jiao Tong University, Shanghai 200240, China*

*Collaborative Innovation Center of IFSA, Shanghai Jiao Tong University, Shanghai 200240, China*

---

## Abstract

We investigate isospin-symmetry breaking effects in the  $sd$ -shell region with large-scale shell-model calculations, aiming to understand the recent anomalies observed in superallowed Fermi  $\beta$ -decay. We begin with calculations of Coulomb displacement energies (CDE's) and triplet displacement energies (TDE's) by adding the  $T = 1, J = 0$  isospin nonconserving (INC) interaction into the usual isospin-invariant Hamiltonian. It is found that CDE's and TDE's can be systematically described with high accuracy. A total number of 122 one- and two-proton separation energies are predicted accordingly, and locations of the proton drip-line and candidates for proton-emitters are thereby suggested. However, attempt to explain the anomalies in the superallowed Fermi  $\beta$ -decay fails because these well-fitted  $T = 1, J = 0$  INC interactions are found no effects on the nuclear matrix elements. It is demonstrated that the observed large isospin-breaking correction in the  $^{32}\text{Cl}$   $\beta$ -decay, the large isospin-mixing in the  $^{31}\text{Cl}$   $\beta$ -decay, and the small isospin-mixing in the  $^{23}\text{Al}$   $\beta$ -decay can be consistently understood by introducing additional  $T = 1, J = 2$  INC interactions related to the  $s_{1/2}$  orbit.

**Keywords:** Isospin-symmetry breaking, Isospin-nonconserving interaction, Superallowed Fermi  $\beta$ -decay, Coulomb displacement energy, Triplet displacement energy, Proton drip-line

**PACS:** 21.10.Sf, 21.30.Fe, 21.60.Cs, 27.50.+e

---

The degeneracies of energy levels in nuclei with interchanging number of protons and neutrons indicate the existence of isospin symmetry [1, 2]. The concept of this approximate symmetry is successful in describing various observables, there are conditions where it does not hold. Isospin symmetry is broken in QCD due to the mass difference between the up and down quarks and their electromagnetic interaction [3]. In nuclei, the Coulomb interaction and the charge-dependent nucleon-nucleon interaction break this symmetry, giving rise to observable effects. Especially for nuclei near the  $N = Z$  line, both the ground states and excited spectra are affected by isospin-

symmetry breaking (ISB). Therefore, investigation of proton-rich nuclei far from the line of stability provides important testing ground for ISB effects. It has been known that ISB in nuclear many-body systems in terms of the isospin nonconserving (INC) interactions [4] leads to non-zero Coulomb displacement energy (CDE) [5, 6] and triplet displacement energy (TDE) (see definitions in Eq. (1) below). While the microscopic origin of possible INC sources is yet to be understood, study of these quantities must involve the knowledge of the many-body effects in nuclear structure [7]. This suggests that the detailed shell-model calculations with an inclusion of INC forces are es-

essential for further refining our knowledge about ISB. Recently, it has been shown that the INC interaction of the  $T = 1, J = 0$  channel plays an important role in the explanation of characteristic behavior of the  $f_{7/2}$ -shell CDE's [8, 9] and TDE's [9]. Mirror energy differences (MED's) [6] and triplet energy differences (TED's) [10, 11] were previously studied in the  $f_{7/2}$ -shell, and have recently been investigated by us for the upper  $fp$ -shell nuclei [12]. On the other hand, for light nuclei the MED's have been discussed in the relation with the loosely bound  $s_{1/2}$  proton [13, 14], which reduces the Coulomb repulsion and hence strongly influences the MED's of the corresponding nuclei [15, 16]. We remark that the MED's in the  $sd$ -shell could have a different origin from that in the  $fp$ -shell.

Superallowed Fermi  $\beta$ -decay serves as a crucial nuclear input to test the precise values of the Cabbibo-Kobayashi-Maskawa (CKM) mixing matrix element  $V_{ud}$  between the  $u$  and  $d$  quarks [17, 18], provided that the radiative and ISB effects are considered properly [19]. In most experiments and theories, the correction due to ISB is known to be smaller than 2% [18, 20, 21], and the nucleus-independent  $\mathcal{F}t$  values are found to be consistent [18]. However, recent data have indicated an anomalously large ISB effect in the superallowed Fermi  $\beta$ -decay of  $^{32}\text{Cl}$  [22] and  $^{31}\text{Cl}$  [23]. An unusually large correction  $\delta_C = 5.3(9)\%$  has been reported for the Fermi  $\beta$ -decay from  $^{32}\text{Cl}$  to the  $T = 1$  isobaric analogue state (IAS) in  $^{32}\text{S}$ , and a large isospin mixing has been observed for the  $\beta$ -decay from  $^{31}\text{Cl}$  to the  $T = 3/2$  IAS in  $^{31}\text{S}$ . It should be noted that these results may depend on both the INC force and the location of the states that mix. An accidental near-degeneracy of the states could enhance isospin mixing, without requiring a particularly strong INC force. This can be estimated by using the perturbation theory, which, subsequently, can be applied to extract the INC mixing matrix element from the experimental data of the superallowed Fermi  $\beta$ -decays [24]. Furthermore, the observation of the strong isospin mixing for  $A = 23$  is still controversial [25, 26]. A consistent understanding of all the above requires detailed shell-model calculations for the  $sd$ -shell region.

In order to understand these anomalies in the superallowed Fermi  $\beta$ -decay, we first investigate CDE's [6] and TDE's [9, 27] for ground and isobaric analogue states in an isospin multiplet of the total isospin  $T$ , with  $T_z = (N - Z)/2$  specifying different states of isospin projection in the multiplet. CDE and TDE are defined as

$$\begin{aligned} \text{CDE}(A, T) &= BE(T, T_{z>}) - BE(T, T_{z>} + p), \\ \text{TDE}(A, T) &= BE(T, T_z = -1) + BE(T, T_z = +1) \\ &\quad - 2BE(T, T_z = 0), \end{aligned} \quad (1)$$

where  $BE(T, T_z)$  are the negative binding energies of ground and isobaric analogue states. Here in the CDE's,  $p$  protons exchange with neutrons, and  $T_{z>}$  is the  $T_z$  for the larger- $Z$  isobar in a mirror pair. From the definitions in Eqs. (1), one sees that while the first quantity resembles differences in mirror binding energies, the second is meaningful only for triplets. In our notation, the total spin and parity  $I^\pi$  of the isobaric multiplets are implicitly included, but omitted in above equations for simplicity.

In Fig. 1(a), the experimental CDE's for the  $sd$ -shell with  $T = -T_{z>} = +1/2, p = 1$  are shown, where the binding energies are those of the ground states of a mirror pair with  $T_z = \pm 1/2$  [28]. The experimental TDE's for the  $sd$ -shell with  $T = 1$  are shown in Fig. 1(b), where  $BE(T, T_z = 0)$  in Eq. (1) is taken as the binding energy of the isobaric analogue state and  $BE(T, T_z = \pm 1)$  are those of the ground states. Both CDE's in Fig. 1(a) and TDE's in Fig. 1(b) are compared with the Coulomb energy prediction with spherical charged distribution (dotted curve) [6]. One can see that the results of the Coulomb contribution for simple homogeneous spherical charge lie far above the CDE data in Fig. 1(a), and in Fig. 1(b-c), the results of charged sphere give only a smooth curve that tends to be the average of the staggerings seen from data.

In order to examine the characteristic patterns of CDE and TDE more clearly, we use quantities measuring differences in CDE's between  $A$  and  $A + 2$  and in TDE's between  $A$  and  $A + 4$  nuclei [9],

$$\begin{aligned} \Delta\text{CDE}(A, T) &= \text{CDE}(A + 2, T) - \text{CDE}(A, T), \\ \Delta\text{TDE}(A, T) &= \text{TDE}(A + 4, T) - \text{TDE}(A, T). \end{aligned} \quad (2)$$

In Fig. 1(c), one begins to see an odd-even staggering pattern in  $\Delta\text{CDE}/Z$ , while the Coulomb energy prediction gives only a smooth average curve. Here by 'odd' and 'even' we refer to the larger proton number ( $Z >$  in Eq. (1)) in a mirror pair with  $A$ . The occurrence of the odd-even staggerings can be explained by the differences between proton- and neutron-pairing gaps [9]. In Fig. 1(b,d), data for TDE and  $\Delta\text{TDE}/Z$  exhibit strong zigzags, particularly strong for the lighter nuclei in the  $sd$ -shell.

In the following, we perform shell-model calculations with the charge-independent interaction USDA [29] ( $H_0$ ) and additional isovector and isotensor  $T = 1, J = 0$  INC interaction ( $H_{INC}$ ). The INC force strengths are fitted to the experimental CDE's and TDE's that are extracted from the binding-energy data of the  $sd$ -shell. After the experimental CDE's and TDE's are described, we then use the more sensitive quantities  $\Delta\text{CDE}/Z$  and  $\Delta\text{TDE}/Z$  to adjust the INC forces finely. The total Hamiltonian is given as

$$H = H_0 + H_{INC}, \quad (3)$$

where  $H_{INC}$  takes the form of a spherical tensor of rank two

$$H_{INC} = H'_{sp} + V_C + \sum_{k=1}^2 V_{INC}^{(k)}, \quad (4)$$

with  $V_C$  being the Coulomb interaction and  $H'_{sp}$  the single-particle Hamiltonian that includes the Coulomb single-particle energies for protons and the single-particle energy shifts  $\epsilon_{ls}$  due to the electromagnetic spin-orbit interaction [30]. The Coulomb single-particle energies for protons are taken as  $\epsilon(d_{5/2}) = 3.60$ ,  $\epsilon(s_{1/2}) = 3.55$ , and  $\epsilon(d_{3/2}) = 3.60$  (all in MeV) for the  $sd$  model space. The two-body matrix elements of the INC interaction  $V_{INC}^{(k)}$  in Eq. (4), with  $k = 1$  and  $k = 2$  for the isovector and isotensor component, respectively, are related to those in the proton-neutron formalism [31, 6] through

$$\begin{aligned} V_{abcd,J}^{(1)} &= V_{abcd,J}^{pp} - V_{abcd,J}^{nn}, \\ V_{abcd,J}^{(2)} &= V_{abcd,J}^{pp} + V_{abcd,J}^{nn} - 2V_{abcd,J}^{pn}, \end{aligned} \quad (5)$$

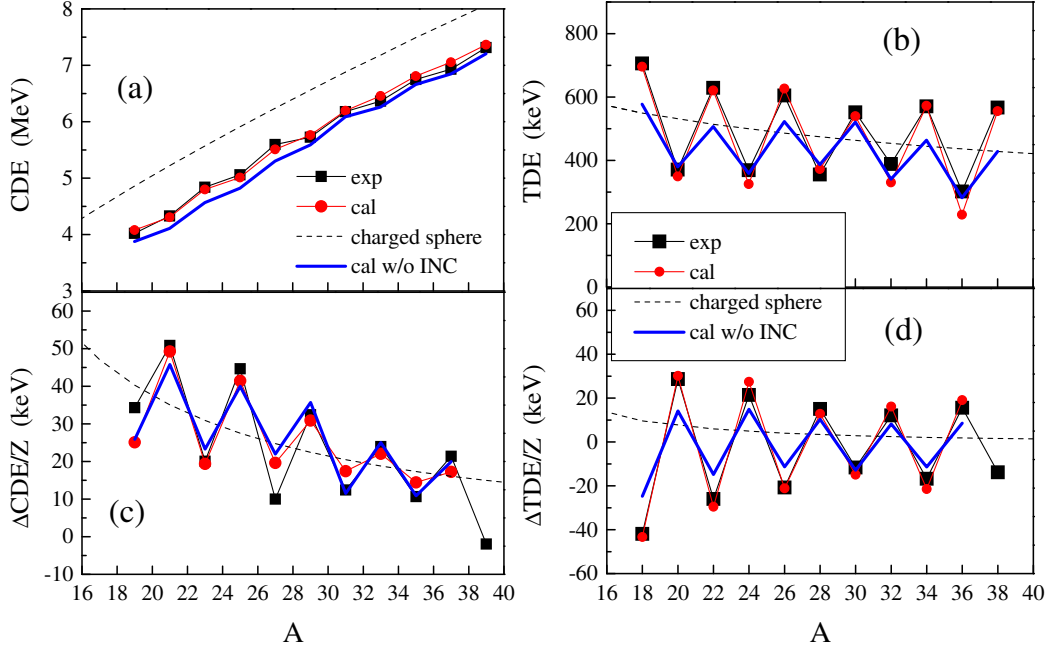


Figure 1: Experimental Coulomb displacement energy and triplet displacement energy. (a) CDE's for  $T = 1/2$ , (b) TDE's for  $T = 1$ , (c) differences in CDE's between  $A$  and  $A + 2$  nuclei (shown as  $\Delta\text{CDE}/Z$ ), and (d) differences in TDE's between  $A$  and  $A + 4$  nuclei (shown as  $\Delta\text{TDE}/Z$ ). Experimental data are taken from Ref. [28]. Theoretical curves from the Coulomb prediction [6] are shown for comparison.

where  $V_{abcd,J}^{pp}$ ,  $V_{abcd,J}^{nn}$ , and  $V_{abcd,J}^{pn}$  are, respectively, the  $pp$ ,  $nn$ , and  $pn$  matrix elements with isospin  $T = 1$  and spin  $J$ . We note that more general two-body charge-dependent interactions have been proposed in Refs. [4, 32, 33].

As our previous treatment for the upper  $fp$  shell region [12], we adopt the INC isovector  $V_{aabb,J=0}^{(1)}$  and isotensor  $V_{aabb,J=0}^{(2)}$  interactions in Eq. (5) with  $T = 1, J = 0$  for each orbit (here  $a, b = d_{5/2}, s_{1/2}, d_{3/2}$ ). Subsequently, only the diagonal interaction matrix elements are considered and off-diagonal ones are neglected. We can simply denote  $V_{J=0}^{(1)}(a) = V_{abcd,J=0}^{(1)}$  and  $V_{J=0}^{(2)}(a) = V_{abcd,J=0}^{(2)}$  with  $a = b = c = d$  in Eqs. (5). The parameters are chosen to be (all in keV)

$$\begin{aligned} V_{J=0}^{(1)}(d_{5/2}) &= 100, & V_{J=0}^{(2)}(d_{5/2}) &= 150, \\ V_{J=0}^{(1)}(s_{1/2}) &= -200, & V_{J=0}^{(2)}(s_{1/2}) &= -190, \\ V_{J=0}^{(1)}(d_{3/2}) &= -100, & V_{J=0}^{(2)}(d_{3/2}) &= 170, \end{aligned} \quad (6)$$

so as to reproduce the experimental CDE and TDE data.

Calculations are performed with the shell model code MSHELL64 [34] for odd-mass nuclei with odd-neutron number and isospin  $T = 1/2, 3/2, 5/2$ , and  $7/2$ , and for even-mass nuclei with  $T = 1, 2$ , and  $3$  in the  $sd$  model space.

Figure 1 shows the calculated results for  $sd$ -shell nuclei with mass  $A = 18 - 39$ . As one can see from Fig. 1(a), the CDE curve calculated without the INC forces lies below the data points. This reconfirms the well-known "Nolen-Schiffer Anomaly" [35], which states that there remains a consistent under-estimate of the CDE's, even after the Coulomb interaction and all the related corrections were taken into account. The calculations with the INC forces clearly shift the curve up to a

point that the theoretical results agree nicely with data. For Fig. 1(c), one may conclude that the  $T = 1, J = 0$  isovector and isotensor INC interactions are not very sensitive to the quantity  $\Delta\text{CDE}/Z$ , because, as one can see from Fig. 1(c), the calculated patterns with and without the INC forces are not very different. However, TDE is found to be a more sensitive probe for the INC interactions. Figure 1(b) depicts that calculations without INC deviate significantly from the data, especially for the upper branch in the staggering pattern (for mass numbers 18, 22, 26, 34, and 38). By including the INC interactions, an excellent agreement with the experimental data for TDE's of the mass region  $A = 18 - 38$  can be obtained, as seen in Fig. 1(b). In Fig. 1(d), the experimental  $\Delta\text{TDE}/Z$  are also better reproduced by considering the INC interactions. The rms deviations between the calculated and experimental CDE's and TDE's are 66 keV and 34 keV, respectively. Thus we have demonstrated, consistent with previous findings [10, 12], that the  $T = 1, J = 0$  INC interactions are important, and seem to be efficient, for describing the characteristic behaviors in CDE's and TDE's of the  $sd$ -shell. Nevertheless, we stress that INC forces with nonzero spin may be needed for the other observations [36], which is the central theme of the next discussion.

To demonstrate that the present shell-model calculations with the chosen effective INC interactions work also for the excited multiplet states in this mass region, we list in Table 1 the CDE's and TDE's for the ground and excited multiplet states in  $A = 22, 23, 29 - 32$ . These mass numbers are chosen because they involve the isotopes of our present interest ( $^{31}\text{Cl}$ ,  $^{32}\text{Cl}$ , and  $^{23}\text{Al}$ ), for which transition strengths in superallowed Fermi  $\beta$ -decay were observed [22, 23, 25], and these will be the main focus

Table 1: Comparison between experimental and calculated CDE and TDE values (in keV) for the ground and excited multiplet states for  $A = 22, 23, 29 - 32$ . All the CDE's are calculated for states with  $T = 1/2, T_{z>} = 1/2, p = 1$  (see Eq. (1)), except for  $I_i^\pi = 3/2_2^+$  in  $A = 31$  with  $T = 3/2, T_{z>} = 1/2, p = 1$ . Experimental data are taken from Ref. [28, 37].

CDE				TDE			
$A$	$I_i^\pi$	expt.	calc.	$A$	$I_i^\pi$	expt.	calc.
23	$3/2_1^+$	4838.4	4798.1	22	$0_1^+$	620.1	620.6
	$5/2_1^+$	4849.7	4806.5		$2_1^+$	555.7	530.0
	$7/2_1^+$	4815.1	4806.6		$4_1^+$	461.1	424.6
29	$1/2_1^+$	5724.8	5763.6	30	$0_1^+$	551.9	539.6
	$3/2_1^+$	5835.0	5835.3		$2_1^+$	476.8	448.6
31	$1/2_1^+$	6179.9	6196.0		$2_2^+$	441.4	416.7
	$3/2_1^+$	6161.6	6179.1	32	$1_1^+$	388.2	332.0
	$5/2_1^+$	6180.3	6168.6		$2_1^+$	328.4	310.6
	$3/2_2^+$	6189.1	6137.4		$0_1^+$	298.4	256.6

of our discussion in the later sections. For example, the CDE of  $A = 31$  with  $I_i^\pi = 3/2_2^+$  shown in Table 1 is calculated for  $T = 3/2, T_{z>} = -1/2, p = 1$  using Eq. (1), which involves the isobaric analogue state of the daughter nucleus  $^{31}\text{S}$  in the Fermi  $\beta$ -decay of  $^{31}\text{Cl}$ , which will be discussed later in Fig. 3(b). As one can see in Table 1, the calculated CDE's and TDE's are in a reasonably good agreement with the experimental data, except for  $A = 32$ , where larger discrepancies are observed.

By combining the shell-model CDE( $A, T$ ) with the experimentally-known  $BE(A, T, T_z = T)$  of the neutron-richer isobars [28],  $BE(A, T, T_z = -T)$  of the corresponding proton-richer isobars can be calculated, and their one- and two-proton separation energies ( $S_p, S_{2p}$ ) can thereby be obtained [9, 8]. Figure 2 shows a total number of 122 one- and two-proton separation energies denoted in each box by the first and second numbers, respectively. Among them, 72 have data to compare with and 50 are our predictions. We have found that the calculated and experimental one- and two-proton separation energies agree very well within a rms deviation of about 94 keV and 148 keV, respectively. Without the  $T = 1, J = 0$  INC force in the calculation, the rms deviations for  $S_p$  and  $S_{2p}$  increase by 18.5 keV and 30.9 keV, respectively. It is to be noted that several proton-rich nuclei, for example  $^{26,27}\text{S}$ ,  $^{30}\text{Ar}$ , and  $^{34,35}\text{Ca}$ , however, exhibit large discrepancies by about 200 keV. The thick (red) lines represent the proton drip-line beyond which the one-proton and/or two-proton separation energies become negative. Figure 2 also suggests several candidates for proton emitters in the  $sd$ -shell mass region. Consistent with our results, two new proton-unbound isotopes  $^{30}\text{Ar}$  and  $^{29}\text{Cl}$  have recently been identified, pointing to a violation of isobaric symmetry in the structure [38].

Fermi  $\beta$ -decay provides one of the critical observations to probe isospin symmetry, which leads to strict selection rules for superallowed Fermi transition with the matrix element  $M_0$  corresponding to the isospin symmetry. However, due to ISB, the Fermi matrix element for the transition is modified as  $|M_F|^2 = |M_0|^2(1 - \delta_C)$ , where  $\delta_C$ , called isospin-breaking correction, is expected to contain all the symmetry-breaking effects [18], and is known to be smaller than 2%. For theoretical calculations,

the model space has to be very large because, in the first place, the Coulomb force is long range in nature. Calculations in a large shell-model space are not possible due to huge dimensions of configuration. Hardy and Towner [17, 18] thus wisely divided  $\delta_C$  into two parts,  $\delta_C = \delta_{C1} + \delta_{C2}$ , where  $\delta_{C1}$  arises from configuration mixing in a restricted shell-model space and  $\delta_{C2}$  separately contributes from the mixing with outside, which is estimated by computing radial overlap integrals with proton and neutron radial functions [18].

Recently, it has been reported [22] that the isospin-breaking correction  $\delta_C = 5.3(9)\%$  for the observed  $ft = 3200(30)\text{s}$  in the Fermi transition from  $^{32}\text{Cl}$  to  $^{32}\text{S}$  is anomalously larger than the typical values observed in many other superallowed decays [18]. It has been suggested that the closely-lying excited  $T = 1, I^\pi = 1^+$  and  $T = 0, I^\pi = 1^+$  states with the energy separation  $188.2 \pm 1.2$  keV [22] in  $^{32}\text{S}$  greatly enhances the isospin mixing, and also the isospin-breaking correction [22]. In another very recent work [23], a large isospin mixing has been observed in  $^{31}\text{Cl}$   $\beta$  delayed  $\gamma$ -decay experiment. The investigation indicates a large isospin-mixing between the  $T = 1/2$  and  $T = 3/2$  states with spin-parity  $I^\pi = 3/2^+$ . The matrix element of the Fermi transition between  $^{31}\text{Cl}$  and  $^{31}\text{S}$  has been observed as  $|M_F|^2 = 2.4(1)$  for  $T = 3/2$  and  $|M_F|^2 = 0.48(3)$  for  $T = 1/2$ , while the symmetry-limit values are  $|M_0|^2 = 3$  for  $T = 3/2$  and  $|M_0|^2 = 0$  for  $T = 1/2$ , suggesting a considerable isospin mixing. On the other hand, an early  $^{23}\text{Al}$   $\beta^+$ -decay experiment [25] populated the  $T = 3/2$  IAS in  $^{23}\text{Mg}$  with a  $\log ft$  of 3.31(3), corresponding to  $|M_F|^2 = 3.0$ . In contrast to the two experiments [22, 23] mentioned above, the  $^{23}\text{Al}$   $\beta^+$ -decay result suggests no isospin-mixing.

To understand these experimental data, Fermi matrix elements  $|M_F|^2$  are calculated.  $\delta_{C1}$  can then be obtained from  $\delta_{C1} = 1 - |M_F|^2/|M_0|^2$ , where  $|M_0|^2 = 2$  and  $|M_0|^2 = 3$  for  $T = 1$  and  $T = 3/2$ , respectively. With the  $T = 1, J = 0$  INC interactions, the calculated Fermi transition matrix elements for  $^{32}\text{Cl} \rightarrow ^{32}\text{S}$  and  $^{31}\text{Cl} \rightarrow ^{31}\text{S}$  yield almost  $|M_F|^2 = 2$  and 3, respectively, very close to the symmetry-limit values. These results are totally unexpected. Thus we must answer the question why the superallowed Fermi transitions cannot be described by





tal data ( $\delta_C = 5.3(9)\%$ ) remarkably well. For the  $^{31}\text{Cl}$   $\beta$ -decay calculated with  $V_s = 100$  keV, our results show  $|M_F|^2 = 2.49$  for  $T = 3/2$  and  $|M_F|^2 = 0.47$  for  $T = 1/2$ , as seen in Fig. 3 (b), which are also in good agreement with the experiments. For the  $^{23}\text{Al}$   $\beta^+$ -decay, the calculated value is  $|M_F|^2 = 2.97$ , which indicates a  $\log ft$  of 3.32. Thus the same calculation (with inclusion of the additional isovector and isotensor  $T = 1, J = 2$  INC interactions related to the  $s_{1/2}$  orbit and the same strength  $V_s$ ) also reproduces correctly the experimental suggested small isospin mixing in  $^{23}\text{Al}$ .

With the good description of the superallowed Fermi transition data, we can further use the perturbation theory to estimate the isospin admixture in a two-level mixing model, with the mixed states expressed by

$$\begin{aligned} |\Psi_a\rangle &= \cos\theta|\text{IAS}\rangle + \sin\theta|\text{nonIAS}\rangle, \\ |\Psi_b\rangle &= -\sin\theta|\text{IAS}\rangle + \cos\theta|\text{nonIAS}\rangle. \end{aligned} \quad (7)$$

In Eqs. (7),  $|\text{IAS}\rangle$  and  $|\text{nonIAS}\rangle$  are the isobaric-analogue and non-isobaric-analogue states, respectively, and  $\theta$  is the mixing angle. Following Ref. [24], the mixing matrix element  $v = \langle \text{IAS} | V_{\text{INC}} | \text{nonIAS} \rangle$  can be obtained as  $v = \Delta E \sin(2\theta)/2$  from  $\tan^2\theta = |M_F|_b^2/|M_F|_a^2$  and the energy separation  $\Delta E$  between IAS and non-IAS states. For the  $^{31}\text{Cl}$  decay, our calculated value  $v = 30$  keV compares well with the experimental result  $v = 41$  keV. For the  $^{32}\text{Cl}$  decay, our value  $v = 37.6$  keV agrees remarkably with the experimental one  $v = 36.8$  keV. We can thus conclude that  $T = 1, J = 2$  INC interactions with a single parameter can consistently be used to understand the puzzling observations in superallowed Fermi transition.

The above results have demonstrated the importance of nuclear structure issues apart from the INC force itself. Nuclei with different orbit-occupations may feel the INC force differently. In the  $^{31}\text{Cl}$  and  $^{32}\text{Cl}$   $\beta$ -decays, the occupation of transformed protons in the  $d_{3/2}$  orbit decreases due to the  $T = 1, J = 2$  INC interaction. This influences the Fermi beta-decay transitions by suppressing the Fermi matrix elements  $|M_F|^2$  from 3.0 to 2.49 for the  $^{31}\text{Cl}$  decay and from 2.0 to 1.91 for the  $^{32}\text{Cl}$  decay. For the  $^{23}\text{Al}$  decay, however, the transformed protons from the last occupied  $d_{5/2}$  orbit are affected very little by the  $T = 1, J = 2$  INC interaction, and therefore, the ISB effect becomes negligibly small. Thus the same calculation can consistently explain why the ISB effect is large for  $^{31}\text{Cl}$  but small for  $^{23}\text{Al}$ .

We point out that the present calculations involve free parameters. Although the Coulomb single-particle energies and each term in Eq. (6) have well-defined meanings, the strengths are determined phenomenologically by fitting to data. It is very much desired to understand the origin of the parameters, which should be investigated with realistic forces that properly contain the isospin-violating components.

In summary, we have investigated the effects of isospin non-conserving forces on Coulomb displacement energy, triplet displacement energy, and superallowed Fermi  $\beta$ -decay by performing detailed shell-model calculations for the  $sd$ -shell region. The isospin-invariant USDA effective interaction, together with the Coulomb plus the  $T = 1, J = 0$  isospin-nonconserving forces are employed. We have shown that with

a few fitted INC strengths, the experimental CDE and TDE data of the entire mass region can be described with high accuracy. We conclude that the INC force is important for the  $sd$ -shell and inclusion of the  $T = 1, J = 0$  INC force seems to be sufficient for the description of CDE and TDE. Based on the CDE calculation, we have further calculated a total of 122 one- and two-proton separation energies of the  $sd$ -shell mass region. We have explicitly shown the location of proton drip-lines and suggested potential candidates for proton emitters. However, the calculation with the zero-spin INC force could not explain the three superallowed Fermi  $\beta$ -decay experiments in  $^{31}\text{Cl}$ ,  $^{32}\text{Cl}$ , and  $^{23}\text{Al}$  [22, 23, 25]. We have demonstrated finally that these existing anomalies found in the superallowed  $\beta$ -decay experiments can only be understood with additional  $T = 1, J = 2$  INC interaction that acts between the  $d_{5/2}$  proton and the  $s_{1/2}$  neutron orbit. We have found that the calculated mixing matrix elements by shell model are in good agreement with the experimentally extracted ones for the  $^{31}\text{Cl}$  and  $^{32}\text{Cl}$  decays, and thus we conclude that the anomalous behaviors in the superallowed  $\beta$ -decay can be understood by the level mixing due to the  $T = 1, J = 2$  INC force.

Research at Shanghai Jiao Tong University was supported by the National Key Research and Development Program (No. 2016YFA0400501), the National Natural Science Foundation of China (No. 11575112), and the 973 Program of China (No. 2013CB834401).

## References

- [1] W. Heisenberg, Z. Phys. **77** (1932) 1.
- [2] E. Wigner, Phys. Rev. **51** (1937) 106.
- [3] G. A. Miller, A. K. Oppen, and E. J. Stephenson, Annu. Rev. Nucl. Part. Sci. **56** (2006) 253.
- [4] W. E. Ormand and B. A. Brown, Nucl. Phys. **A491** (1989) 1.
- [5] J. Jäneke, Phys. Rev. **147** (1966) 735.
- [6] M. A. Bentley and S. M. Lenzi, Prog. Part. Nucl. Phys. **59** (2007) 497.
- [7] M. A. Bentley, Nucl. Phys. News **22** (2012) 13.
- [8] B. A. Brown, R. R. C. Clement, H. Schatz, A. Volya, and W. A. Richter, Phys. Rev. C **65** (2002) 045802.
- [9] K. Kaneko, Y. Sun, T. Mizusaki, and S. Tazaki, Phys. Rev. Lett. **110** (2013) 172505.
- [10] A. P. Zuker, S. M. Lenzi, G. Martinez-Pinedo, and A. Poves, Phys. Rev. Lett. **89** (2002) 142502.
- [11] P. E. Garrett *et al.*, Phys. Rev. Lett. **87** (2001) 132502.
- [12] K. Kaneko, T. Mizusaki, Y. Sun, S. Tazaki, and G. de Angelis, Phys. Rev. Lett. **109** (2012) 092504.
- [13] R. G. Thomas, Phys. Rev. **88** (1952) 1109.
- [14] J. B. Ehrman, Phys. Rev. **81** (1951) 412.
- [15] K. Ogawa, H. Nakada, S. Hino, and R. Motegi, Phys. Lett. B **464** (1999) 157.
- [16] C. Yuan, C. Qi, F. Xu, T. Suzuki, and T. Otsuka, Phys. Rev. C **89** (2014) 044327.
- [17] J. C. Hardy and I. S. Towner, Phys. Rev. C **71** (2005) 055501; **79** (2009) 055502.
- [18] I. S. Towner and J. C. Hardy, Phys. Rev. C **77** (2008) 025501.
- [19] W. J. Marciano and A. Sirlin, Phys. Rev. Lett. **96** (2006) 032002.
- [20] B. Hyland, *et al.*, Phys. Rev. Lett. **97** (2006) 102501.
- [21] W. Satula, J. Dobaczewski, W. Nazarewicz, and M. Rafalski, Phys. Rev. Lett. **106** (2011) 132502.
- [22] D. Melconian, *et al.*, Phys. Rev. Lett. **107** (2011) 182301.
- [23] M. B. Bennett, *et al.*, Phys. Rev. Lett. **116** (2016) 102502.
- [24] V. Tripathi, *et al.*, Phys. Rev. Lett. **111** (2013) 262501.
- [25] V. E. Jacob, *et al.*, Phys. Rev. C **74** (2006) 045810.
- [26] R. J. Tighe, *et al.*, Phys. Rev. C **52** (1995) R2298.

- [27] W. Satula, J. Dobaczewski, M. Konieczka, and W. Nazarewicz, *Acta Phys. Pol. B* **45**, 167 (2014).
- [28] M. Wang, *et al.*, *Chin. Phys. C* **36** (2012) 1603.
- [29] B. A. Brown and W. A. Richter, *Phys. Rev. C* **74** (2006) 034315.
- [30] L.-L. Andersson *et al.*, *Phys. Rev. C* **71** (2005) 011303.
- [31] W. E. Ormand, *Phys. Rev. C* **55** (1997) 2407.
- [32] S. Nakamura *et al.*, *Nucl. Phys. A* **575** (1994) 1.
- [33] Y. H. Lam, N. A. Smirnova, and E. Caurier, *Phys. Rev. C* **87** (2013) 054304.
- [34] T. Mizusaki, N. Shimizu, Y. Utsuno, and M. Honma, code MSHELL64 (unpublished).
- [35] J. A. Nolen and J. P. Schiffer, *Annu. Rev. Nucl. Sci.* **19** (1969) 471.
- [36] M. A. Bentley, S. M. Lenzi, S. A. Simpson, and C. Aa. Diget, *Phys. Rev. C* **92** (2015) 024310.
- [37] National Nuclear Data Center, <http://www.nndc.bnl.gov/>.
- [38] I. Mukha, *et al.*, *Phys. Rev. Lett.* **115** (2015) 202501.